MOCVD Growth of Gallium Sulfide Using Di-*tert*-butyl Gallium Dithiocarbamate Precursors: Formation of a Metastable Phase of GaS

Andrea Keys,[1a] Simon G. Bott,[1b] and Andrew R. Barron*,[1a]

*Department of Chemistry, Rice University, Houston, Texas 77005, and
Department of Chemistry, University of Houston, Houston, Texas 77204*

Received June 8, 1999. Revised Manuscript Received September 16, 1999

The reaction of $[(^tBu)_2Ga(\mu\text{-}Cl)]_2$ with 1 molar equiv of $Na(S_2CNR_2)$ yields the di-*tert*-butyl gallium dithiocarbamate compounds $(^tBu)_2Ga(S_2CNR_2)$, R = Me (**1**), Et (**3**), ^nPr (**5**). The *tert*-butyl gallium bis(dithiocarbamate) compounds $(^tBu)Ga(S_2CNR_2)_2$, R = Me (**2**), Et (**4**), ^nPr (**6**), are formed as minor products. Separation of $(^tBu)_2Ga(S_2CNR_2)$ from $(^tBu)Ga(S_2CNR_2)_2$ may be readily accomplished by sublimation of the former. Compounds **1** and **3** are low melting point solids allowing their ready use as liquid precursors for MOCVD. The vaporization enthalpies (ΔH_v) have been determined, by thermogravimetric methods, for compounds **1**, **3**, **5**, $(^nBu)_2Ga(S_2CNMe_2)$ (**7**), and $(^{sec}Bu)_2Ga(S_2CNMe_2)$ (**8**), and are dependent on both the identity of the substituents on gallium and the dithiocarbamate ligand. An inverse relationship is observed between the ΔH_v and the extent of branching of the gallium alkyl. Compounds **1**−**6** are air stable, but compounds **7** and **8** decompose in humid air. The molecular structures of compounds **1** and **3** have been determined by X-ray crystallography. Gallium sulfide (GaS) thin films have been grown at 375−425 °C by atmospheric pressure metal−organic chemical vapor deposition (AP−MOCVD) using compound **1**. Characterization of the films by wavelength dispersive spectroscopy (WDS) microprobe analysis shows the films to have Ga:S compositions of 1:1 with a low degree of impurities (C < 3%; O < 1%). Gallium-rich films were grown from compound **3** using AP−MOCVD and from compound **1** under reduced pressure. XPS studies of the GaS films additionally show an abundance of N on the surface, which has been confirmed to be present throughout the thin film by SIMS measurements. From X-ray diffraction (XRD) and transmission electron microscopy (TEM), the GaS films were found to be a new distorted hexagonal wurtzite phase (a = 4.590 Å, c = 6.195 Å).

Introduction

Recent publications from our laboratory have been concerned with the chemical vapor deposition (CVD) growth of thin films of gallium and indium chalcogenides.[2−4] The main focus of this work has been the understanding of the structural control exerted by the precursor compound on the phase (structure) of the deposited film. The compounds that have been investigated have been either of the general formula $[(R)M(\mu_3\text{-}E)]_4$ or of the general formula $[(R)_2M(\mu\text{-}ER')]_2$ (M = Ga, In). In both cases molecular control and growth of new[2a,2d] or metastable[3] phases was observed. However,

while several of the compounds studied are air and moisture stable, all are solids which severely limits commercialization due to difficulties in precursor delivery.[5] Since several optoelectronic applications of gallium sulfide do not appear to require specific phases, we have become interested in developing air-stable, liquid precursors to gallium sulfide irrespective of phase.

Several other research groups have investigated the CVD growth of gallium and indium chalcogenides,[6−10] although, as with our early work, the precursor compounds are generally solids and issues of increased volatility have not been the primary goal of these studies. An exception has been the work of O'Brien and co-workers with dithiocarbamate compounds of indium, which has demonstrated that films of In_2S_3 may be readily grown from low melting point or liquid precur-

* To whom correspondence should be addressed (http://python. rice.edu/∼arb/Barron.html).

(1) (a) Rice University. (b) University of Houston,

(2) (a) MacInnes, A. N.; Power, M. B.; Barron, A. R. *Chem. Mater.* **1992**, *4*, 11. (b) MacInnes, A. N.; Power, M. B.; Barron, A. R. *Chem. Mater.* **1993**, *5*, 1344. (c) Shulz, S.; Gillan, E. G.; Rogers, L. M.; Rogers, R.; Barron, A. R. *Organometallics* **1996**, *15*, 4880. (d) Gillan, E. G.; Barron, A. R. *Chem. Mater.* **1997**, *9*, 3037.

(3) (a) MacInnes, A. N.; Cleaver, W. M.; Barron, A. R.; Power, M. B.; Hepp, A. F. *Adv. Mater. Opt. Electron.* **1992**, *1*, 229. (b) MacInnes, A. N.; Power, M. B.; Hepp, A. F.; Barron, A. R. *J. Organomet. Chem.* **1993**, *449*, 95. (c) Stoll S. L.; Barron, A. R. *Chem. Mater.* **1998**, *10*, 650.

(4) Stoll, S. L.; Gillan, E. G.; Barron, A. R. *Chem. Vap. Deposition* **1996**, *2*, 182.

(5) Maury, F. *Chem. Vap. Deposition* **1996**, *2*, 113.

(6) Gysling, H. J.; Wernberg, A. A.; Blanton, T. N. *Chem. Mater.* **1992**, *4*, 900.

(7) Cheon, J.; Arnold, J.; Yu, K.-M.; Bourret, E. D. *Chem. Mater.* **1995**, *7*, 2273.

(8) Nomura, R.; Konishi, K.; Matsuda, H. J. *Electrochem. Soc.* **1991**, *138*, 631.

(9) Bessergenev, V. G.; Bessergenev, A. V.; Ivanova, E. N.; Kovalevskaya, Y. A. J. *Solid State Chem.* **1998**, *137*, 6.

(10) Zheng, G.; Kunze, K.; Hampden-Smith, M. J.; Duesler, E. N. *Chem. Vap. Deposition* **1996**, *2*, 242.
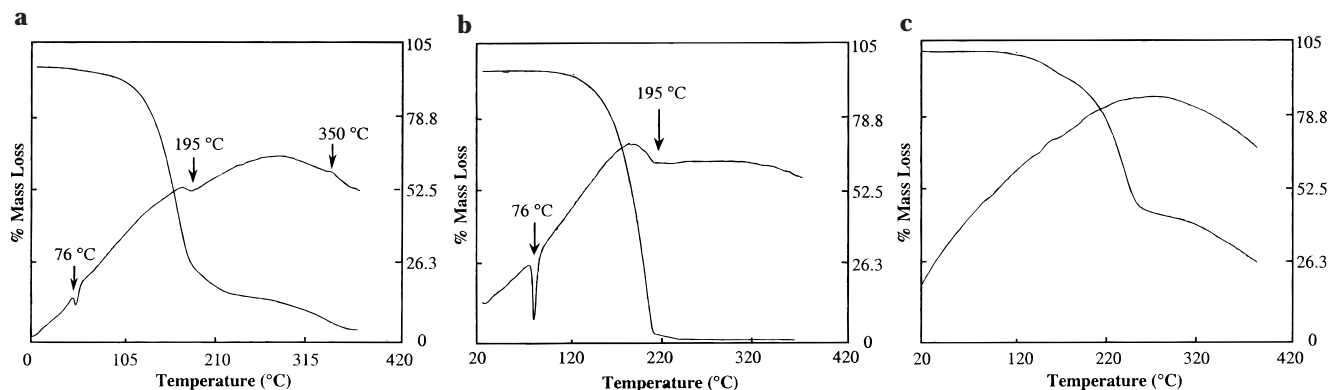
Figure 1. Thermogravimetric/differential thermal analysis (TG/DTA) of (a) the product from the reaction of Na(S$_2$CNMe$_2$) with [(^{t}Bu)$_2$Ga(μ-Cl)]$_2$, and the purified products (b) (^{t}Bu)$_2$Ga(S$_2$CNMe$_2$) (**1**) and (c) (^{t}Bu)$_2$Ga(S$_2$CNMe$_2$) (**2**), respectively.

sors.[11,12] The use of the analogous diselenocarbamate compounds allows for the growth of selenide films.[13,14] However, despite the preparation of a number of dithiocarbamate compounds of gallium (including Ga(S$_2$-CNEt$_2$)$_3$,[11] Ga(S$_2$CN=CC$_4$H$_4$)$_3$,[11] R$_2$Ga(S$_2$CNEt$_2$),[11] and R$_2$Ga[S$_2$CN(Me)CH$_2$CH$_2$CH$_2$NMe$_2$][12]) the growth of gallium sulfide has been generally less successful than that of indium sulfide. In fact little or no film growth was observed using either Et$_2$Ga(S$_2$CNEt$_2$) or (neo-C$_5$H$_{11}$)$_2$-Ga(S$_2$CNEt$_2$).[11] However, the work by O'Brien and co-workers was the initial inspiration for our present study.

In setting out to prepare suitable air-stable, liquid precursors, two general issues must be considered. First, what makes a compound of gallium air stable, and second, how is the volatility of an inorganic or organometallic compound optimized? We have previously shown that four-coordinate compounds of the general formula, [(^{t}Bu)$_2$M(X)]$_n$ (M = Al, Ga, In; X = an anionic ligand), are often inert at the M−C bond, with any reactivity occurring at the M−X bond. To lower the melting points of organogallium compounds, we have confirmed the conventional wisdom, that long chain alkyl groups are beneficial.[15] However, we have also shown that the volatility of a homologous series of organogallium compounds is related to the total number of intermolecular C−H···H−C interactions.[15] Unfortunately, these two effects can be counter to each other. For example, while [(^{t}Bu)Ga(μ_3-S)]$_4$ melts at a higher temperature than [(EtMe$_2$C)Ga(μ_3-S)]$_4$ the former is more volatile; T_{sub} = 94 vs 102 °C. An ideal precursor would therefore be one where the melting point is minimized, but where the added mass and intermolecular interactions make a negligible contribution to the overall mass of the precursor molecule.

Given the stability of the di-*tert*-butyl derivatives of gallium and the suitability of dithiocarbamate ligands for sulfide thin film growth, we proposed that (^{t}Bu)$_2$Ga-(S$_2$CNR$_2$) would be suitably air-stable, volatile precursors for gallium sulfide. The potential advantages of this class of precursors are as follows: First, the preference

for a chelating mode of coordination of the dithiocarbamate ligand[16] will result in monomeric, and hence more volatile, compounds. Second, the *tert*-butyl ligand has a proven ability to provide the air stability and steric bulk to inhibit any medium to strong inter-interactions.[17] Third, the mass of each *tert*-butyl group (57 amu) is significantly less that the parent dithiocarbamate [S$_2$CNMe$_2$]$^-$ (122 amu), thus limiting the total mass of the precursor and enhancing its volatility when compared to the tris(dithiocarbamate) derivatives, Ga-(S$_2$CNR$_2$)$_3$. Fourth, the identity of R may be readily varied to alter the melting point, hopefully without adversely effecting the volatility significantly.

Results and Discussion

Synthesis and Characterization of (^{t}Bu)$_2$Ga(S$_2$-CNR$_2$). Reaction of [(^{t}Bu)$_2$Ga(μ-Cl)]$_2$ with 2 molar equiv of Na(S$_2$CNMe$_2$) yields the mono(dimethyldithiocarbamate) compound, (^{t}Bu)$_2$Ga(S$_2$CNMe$_2$) (**1**). The *tert*-butyl gallium bis(dithiocarbamate) compound, (^{t}Bu)Ga(S$_2$-CNMe$_2$)$_2$ (**2**) is formed as a minor product. On the basis of the ^{1}H NMR spectrum of the crude reaction mixture the relative ratio of compounds **1**:**2** is approximately 8:1. The thermogravimetric/differential analysis (TG/DTA) of the reaction mixture (Figure 1a) shows a sharp endotherm at 76 °C, followed by a broader endotherm at 195 °C accompanied by a mass loss (74%), and a broad exotherm at 350 °C. These observations are consistent with melting (75 °C) and evaporation (bp = 195 °C) of (^{t}Bu)$_2$Ga(S$_2$CNMe$_2$) (**1**) followed by the thermal decomposition of (^{t}Bu)Ga(S$_2$CNMe$_2$)$_2$ (**2**) (353 °C); see below. From the TGA measurements, the relative ratio of compound **1**:**2** is approximately 9:1, consistent with the NMR data. The observation that compound **1** is more volatile than compound **2** suggests that they may be separated by selective sublimation. This is indeed accomplished at 50 °C under vacuum

(11) Haggata, S. W.; Azad Malik, M.; Motevalli, M.; O'Brien, P.; Knowles, J. C. *Chem. Mater.* **1995**, *7*, 716.

(12) Haggata, S. W.; Azad Malik, M.; Motevalli, M.; O'Brien, P. J. *Organomet. Chem.* **1996**, *511*, 199.

(13) O'Brien, P.; Otway, D. J.; Walsh, J. R. *Chem. Vap. Deposition* **1997**, *3*, 227.

(14) McAleese, J.; O'Brien, P.; Otway, D. J. *Chem. Vap. Deposition* **1998**, *4*, 94.

(15) Gillan, E. G.; Bott, S. G.; Barron, A. R. *Chem. Mater.* **1997**, *9*, 796.

(16) The chelate mode of coordination of the dialkyldithiocarabamate ligand is preferred over bridging as a consequence of the small S−C−S angle. Similar effects have been observed for several different metal centers: see for example: (a) Bonamico, M.; Dessy, G.; Mugnoli, A.; Vaciago, A.; Zambonelli, L. *Acta Crystallogr.* **1965**, *19*, 886. (b) Trindade, T.; O'Brien, P.; Zhang, X.; Motevalli, M. *Chem. Mater.* **1997**, *9*, 523. (c) O'Brien, P.; Walsh, J. R.; Watson, I. M.; Motevalli, M.; Henriksen, L. J. *Chem. Soc., Dalton Trans.* **1996**, 2491.

(17) Dithiocarbamate ligands are known to be either unidentate or bidentate in their binding, the bidentate (chelating) lending stability to the metal center in question; see: Greenwood, N. N.; Earnshaw, A. *Chemistry of the Elements*; Butterworth-Heinemann, Ltd.: London, 1995, Chapter 15, p 795.

$(10^{-2}$ Torr), leaving pure compound **2** as a solid. The TGA's of pure compounds **1** and **2** confirms the assignments discussed above, see parts b and c of Figure 1.
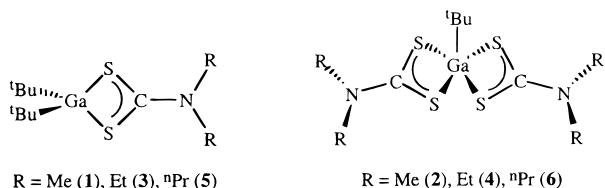
The ethyl and *n*-propyl analogues of compound **1**, $(^{t}Bu)_2Ga(S_2CNR_2)$ [R = Et (**3**) and ^{n}Pr (**5**)], are prepared in a method similar to that of compound **1**. In each case the appropriate bis(dithiocarbamate) compounds, $(^{t}Bu)Ga(S_2CNR_2)_2$, R = Et (**4**), ^{n}Pr (**6**), are also formed as minor products. While compound **3** is readily separated from compound **4** by sublimation, we have been unable to completely separate **5** from **6**. The relative ratio of the mono- to bis(dithiocarbamate) compounds is greater than 8:1 for both **3**:**4** and **5**:**6**.
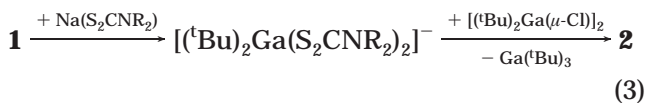
Although compounds **1**, **3** and **5** are the expected metathesis reaction products (eq 1), we propose that the

$$2Na(S_2CNR_2) + [(^{t}Bu)_2Ga(\mu\text{-}Cl)]_2 \rightarrow$$
$$2(^{t}Bu)_2Ga(S_2CNR_2) + 2NaCl \quad (1)$$
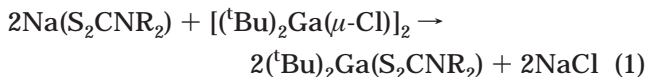
formation of compounds **2**, **4** and **6** is due to a ligand exchange reaction. Once isolated, compounds **1**, **3** and **5** do not convert to their bis(dithiocarbamate) derivatives, precluding the formation of **2**, **4**, and **6** via a ligand exchange reaction, e.g., eq 2. Instead, the observation

$$2(^{t}Bu)_2Ga(S_2CNR_2) \nrightarrow (^{t}Bu)_2Ga(S_2CNR_2)_2 +$$
$$Ga(^{t}Bu)_3 \quad (2)$$
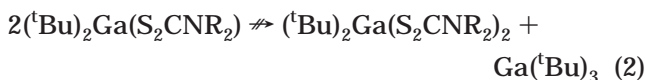
that compounds **2**, **4** and **6** are only formed during synthesis suggests that their formation occurs via an as yet unidentified species, possibly the anionic bis-dithiocarbamate, $[(^{t}Bu)_2Ga(S_2CNR_2)_2]^-$, see eq 3.[18,19]

$$\mathbf{1} \xrightarrow[\text{+ Na(S}_2\text{CNR}_2)]{} [(^{t}Bu)_2Ga(S_2CNR_2)_2]^- \xrightarrow[-\text{ Ga(}^{t}\text{Bu)}_3]{\text{+ [(}^{t}\text{Bu)}_2\text{Ga(}\mu\text{-Cl)]}_2} \mathbf{2}$$
$$(3)$$

The molecular structures of compounds **1** and **3** have been confirmed by X-ray crystallography.[20] The molecular structure of $(^{t}Bu)_2Ga(S_2CNMe_2)$ (**1**) and $(^{t}Bu)_2Ga$-(S_2CNEt_2) (**3**) are shown in Figures 2 and 3; selected bond lengths and angles are given in Table 1. The gallium atoms are in a distorted tetrahedral coordination environment, with the S−Ga−S angle in each compound being significantly smaller than the appropriate C−Ga−C angle as a consequence of the dithocarbamate chelate ring (see Table 1). The structures are similar to the indium compounds, $Me_2In(S_2$-

(18) Leman, J. T.; Barron, A. R.; Ziller, J. W.; Kren, R. M. *Polyhedron* **1989**, *8*, 1909.

(19) We have previously observed that similar species are responsible for diaryltriazenide exchange in indium compounds; see: Leman, J. T.; Roman, H. A.; Barron, A. R. *J. Chem. Soc., Dalton Trans.* **1992**, 2183.

(20) The molecular structure of compound **6** has been reported elsewhere. See: Keys, A.; Bott, S. G.; Barron, A. R. *J. Chem. Cryst.* **1998**, *28*, 629.
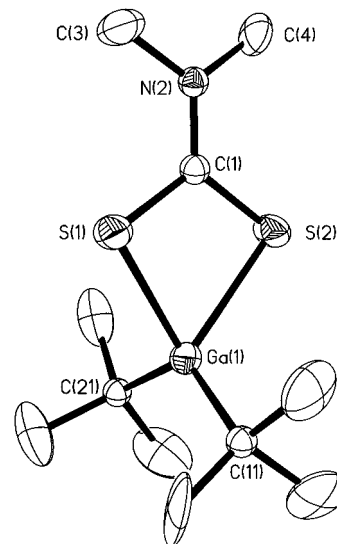
Figure 2. Molecular structure of $(^{t}Bu)_2Ga(S_2CNMe_2)$ (**1**). Thermal ellipsoids are shown at the 30% level, and hydrogen atoms are omitted for clarity.
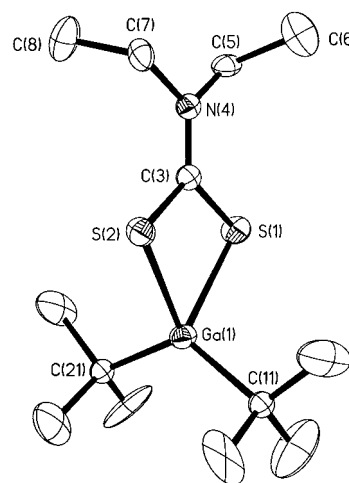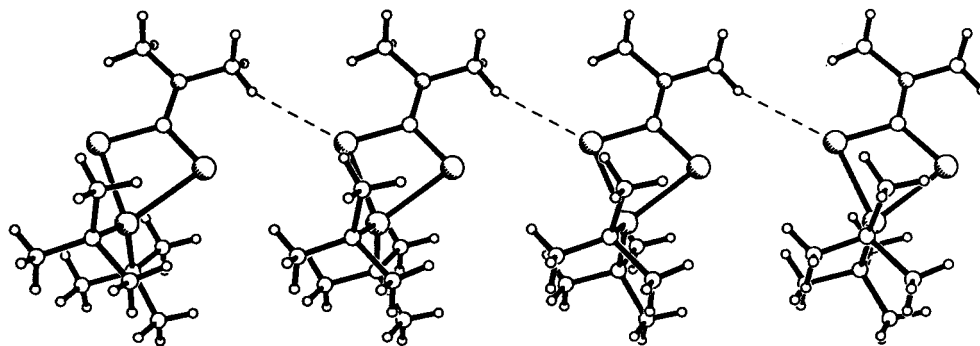

Figure 3. Molecular structure of $(^{t}Bu)_2Ga(S_2CNEt_2)$ (**3**). Thermal ellipsoids are shown at the 30% level, and hydrogen atoms are omitted for clarity.

Table 1. Selected Bond Lengths (Å) and Angles (deg) for $(^{t}Bu)_2Ga(S_2CNR_2)$, R = Me (1) and Et (3)

$(^{t}Bu)_2Ga(S_2CNMe_2)$ (**1**)		$(^{t}Bu)_2Ga(S_2CNEt_2)$ (**3**)	
Ga(1)−S(1)	2.379(5)	Ga(1)−S(1)	2.389(4)
Ga(1)−S(2)	2.425(5)	Ga(1)−S(2)	2.379(4)
Ga(1)−C(11)	1.93(2)	Ga(1)−C(11)	1.97(1)
Ga(1)−C(21)	1.95(2)	Ga(1)−C(21)	1.98(1)
S(1)−C(1)	1.75(2)	S(1)−C(3)	1.71(1)
S(2)−C(1)	1.72(2)	S(2)−C(3)	1.78(1)
N(2)−C(1)	1.30(2)	N(4)−C(3)	1.24(2)
S(1)−Ga(1)-S(1)	74.9(2)	S(1)−Ga(1)-S(1)	75.6(1)
S(1)−Ga(1)-C(11)	109.8(6)	S(1)−Ga(1)-C(11)	111.7(3)
S(1)−Ga(1)-C(21)	109.5(6)	S(1)−Ga(1)-C(21)	110.6(4)
S(2)−Ga(1)-C(11)	114.9(6)	S(2)−Ga(1)-C(11)	113.6(4)
S(2)−Ga(1)-C(21)	110.5(6)	S(2)−Ga(1)-C(21)	110.0(4)
C(11)−Ga(1)-C(21)	125.7(8)	C(11)−Ga(1)-C(21)	124.8(6)
Ga(1)−S(1)-C(1)	85.2(6)	Ga(1)−S(1)-C(3)	85.8(4)
Ga(1)−S(2)-C(1)	84.6(6)	Ga(1)−S(2)-C(3)	84.4(4)
S(1)−C(1)-S(2)	115(1)	S(1)−C(3)-S(2)	113.7(7)
S(1)−C(1)-N(2)	121(1)	S(1)−C(3)-N(4)	124.4(7)
S(2)−C(1)-N(2)	124(1)	S(2)−C(3)-N(4)	121.7(8)

$CNEt_2)$ and $Et_2In(S_2CNEt_2)$, reported by O'Brien and co-workers.[12] Although the chelation of the dithiocarbamate ligand in compound **3** is essentially sym-

Figure 4. View of the intermolecular C−H···S close contact along the crystallographic *b* axis in the crystal structure of (^{t}Bu)$_2$Ga-(S$_2$CNMe$_2$) (**1**).

metrical, that in compound **1** shows a small, but significant, asymmetry; i.e., Ga(1)−S(1) = 2.379(5) Å and Ga(1)−S(2) = 2.425(5) Å. A similar asymmetry has been reported previously of the dithiocarbamate ligands in Ga(S$_2$CNEt$_2$)$_3$ [2.408(2)−2.466(1) Å][21] and the *O*-ethylxanthate ligands Ga(S$_2$COEt)$_3$ [2.405(2), 2.465(2) Å].[22] The reason for this asymmetry is unclear and may possibly be as a consequence of crystal packing forces. A study of the crystal packing diagram of (^{t}Bu)$_2$Ga(S$_2$-CNMe$_2$) (**1**) suggests that the asymmetry in the coordination of the dithiocarbamate ligand is due to C−H···S van der Waals interactions between adjacent molecules (S···H = 2.90 Å; S···C$_{Me}$ = 3.80 Å); see Figure 4. These values are within the sum of the van der Waals radii: S···H = 3.05 Å; S···CH$_3$ = 3.85 Å.[23] Whatever the rationale, it is clear that the dithiocarbamate ligand is flexible enough to accommodate packing forces. Irrespective of any asymmetry in the dithiocarbamate ligand, the average Ga−S bond distances in compounds **1** and **3** would be expected to be shorter than those in the 6-coordinate compounds due to the increased s-orbital character of the Ga−S bond. This is indeed observed. Despite the different Ga−S bond lengths the chelate S−Ga−S angles in **1** [74.9(2)°] and **3** [75.6(1)°] are comparable to that observed for Ga(S$_2$CNEt$_2$)$_3$ [73.38(6), 73.84(4)°],[24] Ga(S$_2$COEt)$_3$ [73.50(6)°],[25] (^{t}Bu)-Ga(S$_2$CN^{n}Pr$_2$)$_2$ [73.30(5) and 72.95(5)°][20] and (^{i}PrO)Ga-(S$_2$CNEt$_2$)$_2$ [73.2(1) and 73.9(1)°].[20] A second unusual distortion is observed in the structure of compounds **1** and **3**; the dithiocarbamate ligand appears to bent away from an idealized C$_{2v}$ symmetry. The gallium atoms lie 0.22 and 0.21 Å above the S$_2$CN plane of the dithiocarbamate ligands in compounds **1** and **3**, respectively. On the basis of the closeness and relative position of adjacent molecules, we propose that this distortion is due to the head-to-tail molecular packing (Figure 5) and not inherent in the structure.

Determination of Vaporization Enthalpies (ΔH$_v$) for (^{t}Bu)$_2$Ga(S$_2$CNR$_2$). To be effective, an MOCVD precursor must exhibit a relatively high volatility in order to be transported to a substrate in a facile manner. To determine the volatilities of **1**, **3**, and **5**, and thus

their suitability as precursors, their relative mass loss over several minutes at constant temperature was determined. An appropriate temperature range was chosen in which the mass loss was due only to vaporization, with no decomposition occurring (100−150 °C). These values were then used to determine vaporization enthalpies (ΔH$_v$) for each compound, based on previously reported methods discussed in detail elsewhere.[15] The general formula is based on the Clausius−Clapeyron relation (eq 4),[26] where ΔH$_v$ is the enthalpy of vaporization, *p* is the vapor pressure, and *R* is the gas constant.

$$d(\ln p)/dT = \Delta H_v/RT^2 \qquad (4)$$

This in combination with the Langmuir equation (eq 5),[27] which relates vapor pressure of a compound to its vaporization rate and gives eq 6 which shows that when the log($m_v T^{1/2}$) is plotted vs $1/T$ the slope gives ΔH$_v$, where M_m is the molecular weight, m_v is the mass loss due to volatilization, and T_v is the volatilization temperature.

$$p = [2\pi RT/M_w]^{1/2} m_v \qquad (5)$$

$$\log (m_v T^{1/2}) = \frac{-0.0522(\Delta H_v)}{T} + \left[\frac{0.0522(\Delta H_v)}{T_v} - \frac{1}{2} \log \left(\frac{1306}{M_w} \right) \right] \qquad (6)$$

Table 2 gives the ΔH$_v$ values calculated for compounds **1**, **3** and **5**, as well as other relevant thermodynamic values.

In considering (^{t}Bu)$_2$Ga(S$_2$CNR$_2$), where R = Me (**1**), Et (**3**), and ^{n}Pr (**5**), the melting point decreases with increased alkyl chain length; i.e., Me > Et > ^{n}Pr. However, the ΔH$_f$ values for compounds **1** and **3** are similar; both being slightly lower than the values for comparably melting organic compounds, for example phenylacetic acid (mp = 76.7 °C, ΔH$_f$ = 14.5 kJ·mol^{-1}) and urethane (mp = 48.7 °C, ΔH$_f$ = 15.2 kJ·mol^{-1}).[28] It would be expected that the boiling points and ΔH$_v$ follow the same trend (i.e., Me > Et < ^{n}Pr); however, this is not observed. Compounds **1** and **5** should have similar boiling points and ΔH$_v$. At this time we do not have an

(21) Dymock, K.; Palenik, G. J.; Slezak, J.; Raston, C. L.; White, A. H. *J. Chem. Soc., Dalton Trans.* **1976**, 28.
(22) Hoskins, B. F.; Tiekink, E. R. T.; Vecchiet, R.; Winter, G. *Inorg. Chim. Acta* **1984**, *90*, 197.
(23) *Handbook of Chemistry and Physics*, 60th ed.; CRC Press: Boca Raton, FL, 1980; p D-194.
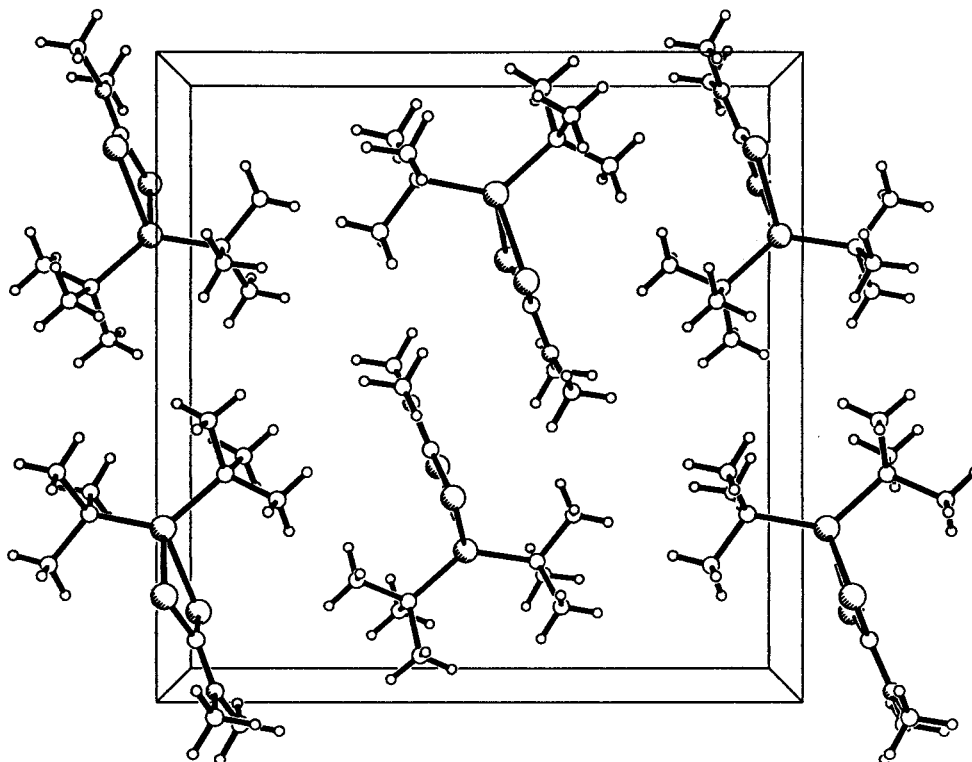(24) Dymock, K.; Pakenik, G. J.; Slezak, J.; Raston, C. L.; White, A. H. *J. Chem. Soc., Dalton Trans.* **1976**, 28.
(25) Delepine, M. *Ann. Chim. (Paris)* **1951**, *6*, 633.

(26) Castellan, G. W. *Physical Chemistry*, 2nd ed.; Addition-Wesley: Menlo Park, CA, 1983; p 268.
(27) Langmuir, I. *Phys. Rev.* **1913**, *2*, 329.
(28) Reference 23, pp C-724−C-731.

Figure 5. Crystal packing structure of $(^tBu)_2Ga(S_2CNMe_2)$ (**1**) showing the presence of close head-to-tail packing of adjacent chains.

Table 2. Thermodynamic Results on $(R)_2Ga(S_2CNR_2)$

compound	mol wt	measd range (°C)	ΔH_f^a (kJ·mol^{-1})	ΔH_v^b (kJ·mol^{-1})	mp^a (°C)	bp^a (°C)
$(^tBu)_2Ga(S_2CNMe_2)$ (**1**)	304	101−152	4.19(1)	43(1)	75	195
$(^tBu)_2Ga(S_2CNEt_2)$ (**3**)	332	99−146	5.43(1)	78(6)	48	203
$(^tBu)_2Ga(S_2CN^nPr_2)$ (**5**)	360	92−151		46(1)		194
$(^nBu)_2Ga(S_2CNMe_2)$ (**7**)	304	112−151		53(1)		269
$(^{sec}Bu)_2Ga(S_2CNMe_2)$ (**8**)	304	93−152		45(1)		240

^{a} From differential thermal analysis (DTA). ^{b} From thermogravimetric analysis (TGA).

Table 3. Reaction Conditions for GaS MOCVD Growth

precursor	deposition temp (°C)	precursor temp. (°C)	pressure (Torr)	Ga:S ratio^a
1	375	80−100	760	51:49
1	400	115−120	760	49:51
1	425	80−90	760	50:50
3	415	60−76	760	61:39
1	350	75−85	0.04^b	79:21

^{a} Determined by microprobe analysis. ^{b} Chamber base pressure prior to deposition run.

explanation for this anomalous behavior. The ΔH_v values for compounds **1**, **3**, and **5** (Table 2) are significantly lower than those reported for simple hydrocarbons of comparable molecular weight, e.g., $C_{22}H_{46}$ (M_w = 310, ΔH_v = 70 kJ·mol^{-1}), $C_{24}H_{50}$ (M_w = 338, ΔH_v = 82 kJ·mol^{-1}), and $C_{25}H_{52}$ (M_w = 352, ΔH_v = 87 kJ·mol^{-1}).[28]

To study the effect of the structure of the gallium's alkyl substituent on volatility, $(^nBu)_2Ga(S_2CNMe_2)$ (**7**) and $(^{sec}Bu)_2Ga(S_2CNMe_2)$ (**8**) were synthesized (see Experimental) and their ΔH_v determined (see Table 2). These results indicate that the more highly branched alkyl group results in a lower ΔH_v, i.e., $^nBu > {^{sec}Bu} \approx {^tBu}$. This is caused by the C−H···H−C van der Waals interactions between the hydrocarbons of adjacent molecules being greater in a straight-chain (linear) substituent (e.g., *n*-butyl) relative to a highly branched (spherical) substituent (e.g., *tert*-butyl). The increased number of C−H···H−C interactions lowers the volatility of the compound. Thus, the highly branched *tert*-butyl group is indeed useful in enhancing the volatility of the MOCVD precursors.

MOCVD of GaS. Both $(^nBu)_2Ga(S_2CNMe_2)$ (**7**) and $(^{sec}Bu)_2Ga(S_2CNMe_2)$ (**8**) are liquids, and thus might be good candidates for gallium sulfide precursors; however,

both decompose upon exposure to air and were therefore not investigated further. Difficulties in purification of $(^tBu)_2Ga(S_2CN^nPr_2)$ (**5**) also precluded study at this time. Thus, we limited our investigations to the MOCVD growth of gallium sulfide films using $(^tBu)_2Ga(S_2CNMe_2)$ (**1**) and $(^tBu)_2Ga(S_2CNEt_2)$ (**3**) as single source precursors. Although solids at room temperature, their low melting points allow for their ready use as liquid sources.

The growth of thin films of gallium sulfide at atmospheric pressure was performed under mild conditions, the precursor **1** being heated to ca. 100 °C over several hours to achieve 0.30−0.65 μm thick films. Table 3 shows the various conditions used for thin film growth. In all but the film grown at 375 °C the as-grown films showed some crystallinity, this exception being amorphous in its initial form. Rates for film growth varied from 0.28 nm·min^{-1} at 375 °C to 0.60 nm·min^{-1} at 425 °C.

Scanning electron microscopy (SEM) and field emission SEM (FESEM) images of the films grown from compound **1** at atmospheric pressure show a very smooth, featureless, uniform surface. To provide a point-of-focus, a film was scratched and the resulting furrow studied; see Figure 6. A smooth "layer" growth is seen
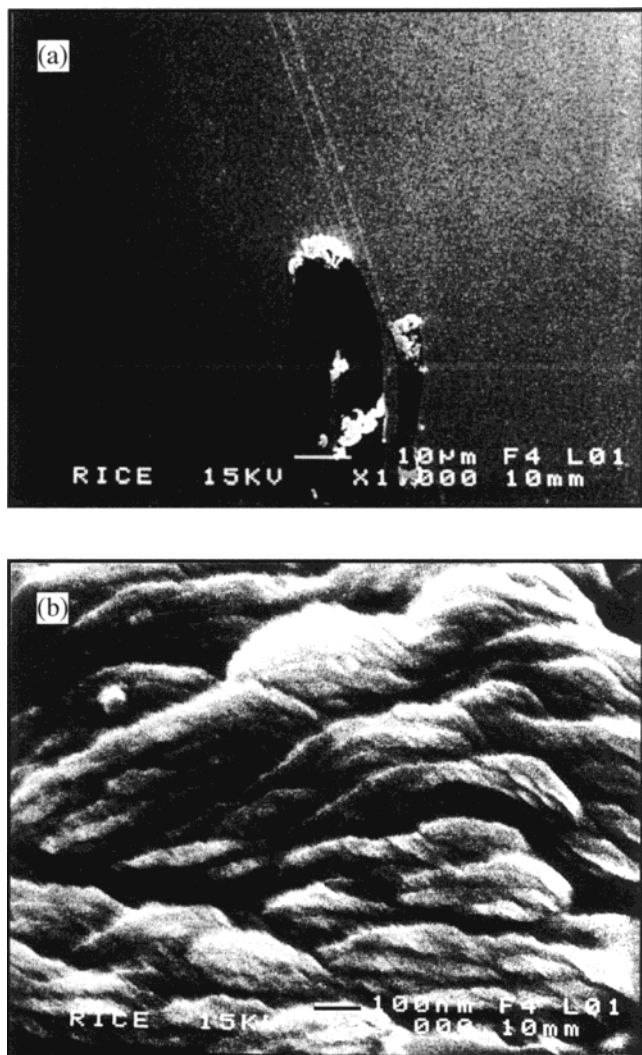
Figure 6. Field emission SEM (FESEM) images of a GaS film grown from (^{t}Bu)$_2$Ga(S$_2$CNMe$_2$) (**1**) at 400 °C by AP−MOCVD, showing (a) a scratch in surface and (b) the end of the furrow.

in transmission electron microscopy (TEM) images of films grown on NaCl plates (see Experimental Section); see Figure 7a, which show an island pattern of growth. Thermal annealing of the films did not provide an increase in surface texture, but additional small cracks in the film indicated the formation of defects due to a mismatch in the thermal coefficient of expansion between the GaS and GaAs substrate.

The X-ray diffraction (XRD) for all the films grown from compound **1**, by AP−MOCVD, were essentially identical; a representative example is shown in Figure 8. No significant changes were observed upon annealing at 600 °C for 5 h. Selected area diffraction (SAD) of the thin films showed the presence of a high degree of crystal orientation (see Figure 7b); some commonalty with the XRD was observed. Neither the XRD or electron diffraction are consistent with the thermodynamically stable hexagonal phase of GaS (JCPS #30−0576) or either of the known metastable rhombohedral[29] or cubic phases.[2] Despite the apparent preferred orientation of the films (see below), the use of the XRD data, in conjunction with the electron diffraction results,
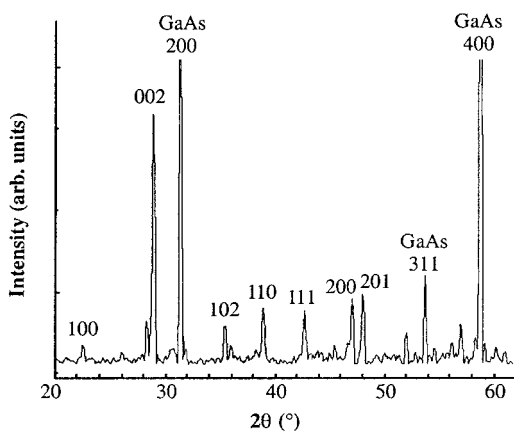
(29) Pardo, M.; Flauhaut, J. *Mater. Res. Bull.* **1987**, *22*, 323.
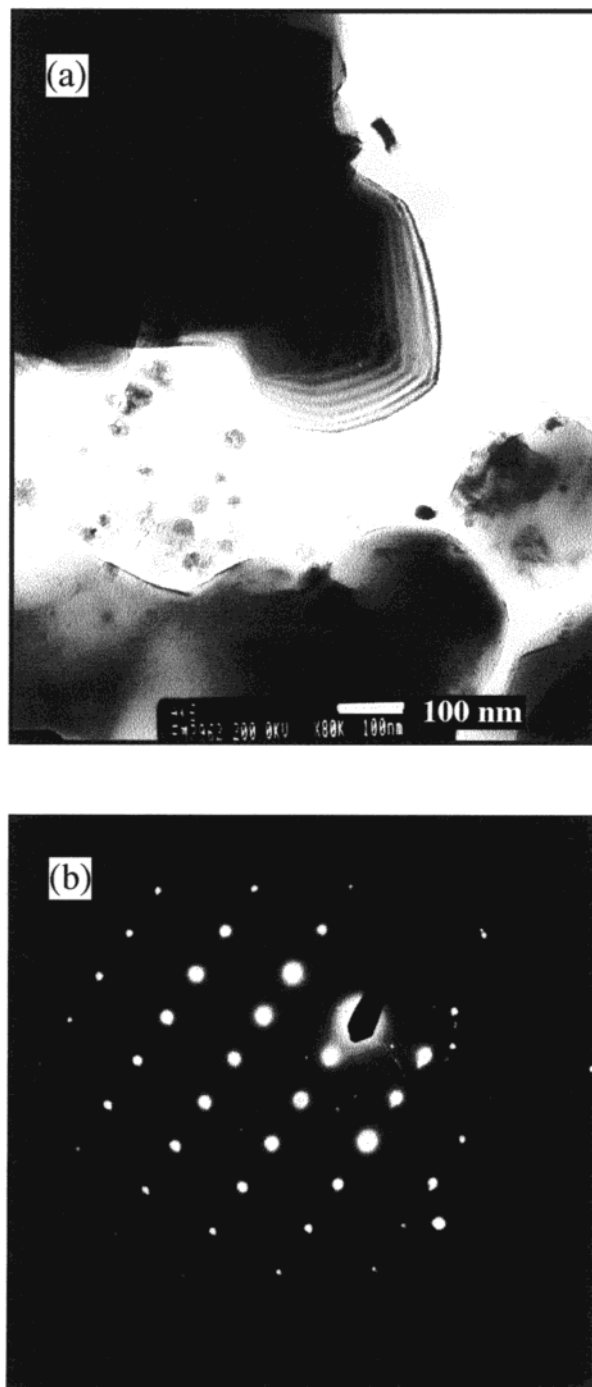
Figure 7. TEM image of a GaS film grown from (^{t}Bu)$_2$Ga-(S$_2$CNMe$_2$) (**1**) at 400 °C by AP−MOCVD (a), showing an island pattern of growth, and its associated selected area electron diffraction patterns (b).

allowed all peaks to be indexed (see Experimental) to a distorted hexagonal wurtzite structure, $a = 4.590$, $c = 6.195$ Å. Table 4 lists the experimental and calculated d spacing for this structure.

Although the observation of a wurtzite phase for GaS is new, wurtzite-type structures are known for other stoichiometries of gallium sulfide. Both α-Ga$_2$S$_3$ and β-Ga$_2$S$_3$ have wurtzite type structures, with ordered and disordered vacancies, respectively. However, only β-Ga$_2$S$_3$ has a hexagonal lattice; α-Ga$_2$S$_3$ being monoclinic.[30] The lattice constants for β-Ga$_2$S$_3$ ($a = 3.678$, $c = 6.016$ Å) are similar, but smaller, to the lattice constants found in this study.[31] We have previously reported that the

Figure 8. Representative XRD of a GaS film grown from (ᵗBu)₂Ga(S₂CNMe₂) (**1**) at 400 °C by AP−MOCVD. Peaks due to the GaAs substrate are labeled.

Table 4. Measured *d* Spacing (Å) for GaS Films Grown from (ᵗBu)₂Ga(S₂CNMe₂) (1) Compared to Calculated Values for Wurtzite Lattice and β-Ga₂S₃

hkl	I/I_0	exptl	calcd	β-Ga₂S₃
100	7.0	4.00[a,b]	3.975	3.185
101		3.34[b]	3.346	2.815
002	100	3.10	3.098	3.008
102	17	2.50[a,b]	2.443	2.187
110	20	2.31	2.295	1.839
111	19	2.12	2.152	1.750
200	23	1.93	1.988	1.593
201	25	1.89	1.893	1.540
203	−	1.43[b]	1.432	1.247

[a] XRD and electron diffraction. [b] Electron diffraction.

Table 5. Comparison of Lattice Parameters for Cubic (zinc blende) and Hexagonal (wurtzite) Structures of GaS, Ga₂S₃ and ZnS

	phase		
	cubic (zinc blende)	hexagonal (wurtzite)	
substance	*a* (Å)	*a* (Å)	*c* (Å)
GaS	5.5	4.590	6.195
Ga₂S₃	5.17	3.678	6.016
ZnS	5.410	3.822	6.260

lattice parameter of cubic-GaS (5.5 Å) is larger than that of cubic-Ga₂S₃ (5.17 Å). The increase in size may be rationalized by the increased occupancy of tetrahedral sites from ¹/₃ in Ga₂S₃ to ¹/₂ in GaS. A similar change should be observed for the wurtzite analogues, and as may be seen from Table 5, this trend is indeed present between wurtzite-GaS and β-Ga₂S₃. Furthermore, given the adjacent position of Ga and Zn the cell parameter for cubic-GaS would be expected to be the same or slightly larger. This is indeed observed; see Table 5.

As can be seen from Table 4, the 001 peak in the XRD pattern of GaS grown from compound **1** is the most intense, indicating a preferential orientation in the 001 direction. This pattern was very similar to that found by O'Brien and co-workers[32] in which their Wurtzite ZnS film grown from a dithiocarbamate single-source

precursor was hexagonal wurtzite with preferential orientation in the 001 direction. The use of similar ligands in MOCVD growth in both cases must influence the resultant phase of the thin film, as indicated by the preferred orientation found in both cases regardless of substrate since the O'Brien study used glass as a substrate, while our current substrates were single-crystal GaAs. It should be noted that we have previously reported that preferred orientation hexagonal-GaSe and GaTe films may be grown irrespective of the structure of the substrate.[2d]

Thin films grown, using compound **1**, under low-pressure MOCVD (LP−MOCVD) conditions showed a large excess of gallium to be present, as determined by microprobe analysis (see Table 3). The excess gallium is thought to be metallic gallium deposited amorphously in addition to the GaS, as has been seen with other dithiocarbamate gallium compounds.[33] X-ray diffraction of the gallium sulfide which did form had the same pattern as that found in the atmospheric pressure grown samples, and it was crystalline prior to annealing.

Studies using (ᵗBu)₂Ga(S₂CNEt₂) (**3**) as the MOCVD precursor gave films which appeared similar to those observed from compound **1**, the conditions for film growth being similar in both cases. However, quantitative analysis by wavelength dispersive spectroscopy (WDS) showed the presence of excess Ga in these films, Table 3, which was thought to be amorphous gallium metal. It is unclear how the change from methyl to ethyl (**1** vs **3**) at a site so remote from the reaction center should so drastically alters the mechanism.

XPS and SIMS Analysis. Although WDS analysis showed that the films grown from (ᵗBu)₂Ga(S₂CNMe₂) (**1**) were bulk GaS, we also performed XPS measurements to analyze the surface composition. Measurements were initially achieved at room temperature. In addition to the expected gallium and sulfur (also amounts of carbon and oxygen present), significant quantities (28 atomic %) of nitrogen were observed.[34] A least-squares fit of the N₁ₛ peak indicated the presence of three types of nitrogen-containing species; see Figure 9a. The major peak (63%) at 400.6 eV, has a binding energy similar to the values found for dithiocarbamate ligands bound to various metals, 399.2−400.0 eV.[35,36] The other major peak in this region (29%) has a binding energy of 397.6 eV, which is similar to that reported for bulk GaN (397.0 eV).[37] Heating the sample to 600 °C, in situ, resulted in the disappearance of the dithiocarbamate N₁ₛ peak, leaving the nitride-like material as the predominant nitrogen species, Figure 9b.

Secondary ion mass spectrometry (SIMS) depth profile experiments confirmed the presence of nitrogen throughout the samples. This confirms that the presence of nitrogen must be due to the dithiocarbamate ligand and that the incorporation of nitrogen occurs during the CVD reaction, rather than surface adsorption of atmospheric nitrogen.

(30) *Semiconductors: Other than Group IV Elements and III−V Compounds*; Madelung, O., Poerschke, R., Eds.; Springer-Verlag: Berlin, 1992; p 53.
(31) The Ga−S distances in α-Ga₂S₃ (2.398 Å) and β−Ga₂S₃ (2.256 Å) are similar to the value calculated for the wurtzite GaS (2.323 Å).
(32) Motevalli, M.; O'Brien, P.; Walsh, J. R.; Watson, I. M. *Polyhedron* **1996**, *15*, 2801.
(33) Haggata, S. W.; Azad Malik, M.; Motevalli, M.; O'Brien, P. *Chem. Mater.* **1995**, *7*, 716.
(34) Nitrogen cannot be detected by the WDS system employed in the present study.
(35) Furlani, C.; Polzonetti, G.; Preti, C.; Tosi, G. *Inorg. Chim. Acta* **1983**, *73*, 105.
(36) Polzonetti, G.; Preti, C.; Tosi, G. *Polyhedron* **1986**, *5*, 1969.
(37) Hedman, J.; Martensson, N. *Phys. Scr.* **1980**, *22*, 176.
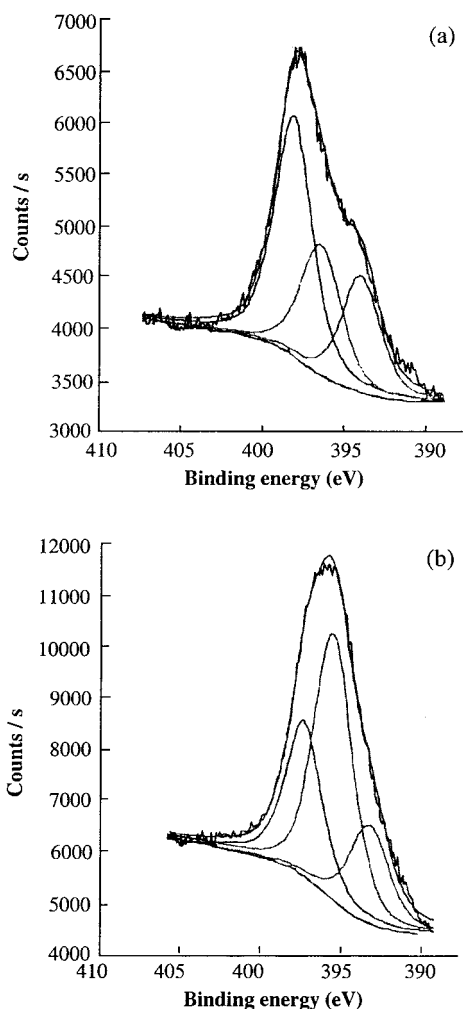
Figure 9. N_{1s} X-ray photoelectron spectra (monochromatized Al-K_{α} radiation) of GaS film grown from (^{t}Bu)$_2$Ga(S$_2$CNMe$_2$) (**1**) at 375 °C (a) before and (b) after in situ annealing.

Conclusions

We have reported the synthesis and structural characterization of low melting point gallium dithiocarbamate compounds, (^{t}Bu)$_2$Ga(S$_2$CNR$_2$). On the basis of the determination of vaporization enthalpies (ΔH_v) for a series of dialkylgallium dithiocarbamate compounds, the highly branched *tert*-butyl group is indeed useful in enhncing the volatility of the MOCVD precursors. AP–MOCVD growth of GaS using (^{t}Bu)$_2$Ga(S$_2$CNMe$_2$) as a single source precursor does not result in the formation of the thermodynamic hexagonal layered phase, but instead a new metastable hexagonal Wurtzite phase is formed. The formation of this metastable phase from a monomeric precursor is contrary to our previous results for cubic-GaS, where the structure of the precursor defined the structure of the deposited phase. However, based on our previous results for the growth of metastable hexagonal-GaTe in which the precursor decomposition mechanism controls the deposited phase, we propose that a similar mode of structural control is present in the system discussed herein. Finally, the use of dithiocarbamate complexes as single source precursors in MOCVD is extensive. In the majority of cases no effort was made to determine the presence of nitrogen in the films. Although, researchers are ordinarily concerned with carbon contamination from or-

ganometallic precursors, we caution against the use of nitrogen-containing ligands such as dithiocarbonate that may result in unwanted nitrogen contamination.

Experimental Section

All operations were carried out using Schlenk techniques or in an argon atmospheric VAC glovebox. NMR spectra were obtained on Bruker AM-250 and Avance 200 spectrometers using (unless otherwise stated) benzene-d_6 solutions. Chemical shifts are reported relative to internal solvent resonances. Mass spectral analysis was obtained on a Finnegan MAT250 mass spectrometer with an electron beam energy of 70 eV for EI mass spectra. IR analysis was carried out on a Nicolet 760 FT-IR spectrometer using Nujol mulls or neat samples in the case of liquids. Melting points were determined using a Seiko TG/DTA 200 thermogravimetric analyzer. Na(S$_2$CNMe$_2$) and Na(S$_2$CNEt$_2$) (Aldrich, 98%) were dried under vacuum (10^{-2} Torr) prior to use. The syntheses of Li[S$_2$CN(^{n}Pr)$_2$][38] Ga(^{t}Bu)$_3$,[39] [(^{n}Bu)$_2$Ga(μ-Cl)]$_2$,[40] [(^{sec}Bu)$_2$Ga(μ-Cl)]$_2$,[40] and [(^{t}Bu)$_2$Ga(μ-Cl)]$_2$[41] were performed by literature methods. All solvents were dried and degassed prior to use.

Synthesis of (^{t}Bu)$_2$Ga(S$_2$CNMe$_2$) (1) and (^{t}Bu)Ga-(S$_2$CNMe$_2$)$_2$ (2). To a slurry of Na(S$_2$CNMe$_2$) (1.58 g, 11.0 mmol) in hexane (20 mL), cooled to −78 °C, was added a slurry of [(^{t}Bu)$_2$Ga(μ-Cl)]$_2$ (2.52 g, 11.5 mmol) in hexane (20 mL) with continuous stirring. The mixture was allowed to warm to room temperature and stirred overnight (12 h). The white precipitate (NaCl) was removed by filtration, and the solution was pumped down to remove any residual volatiles. The off-white powder was sublimed at 50 °C under vacuum (10^{-2} Torr) and the sublimate was recrystallized in toluene to give needles of (^{t}Bu)$_2$Ga(S$_2$CNMe$_2$) (**1**). The nonvolatile residue, (^{t}Bu)Ga(S$_2$-CNMe$_2$)$_2$ (**2**), was also isolated.

(^{t}Bu)$_2$Ga(S$_2$CNMe$_2$) (1). Yield: ca. 70%. MS (EI, %): m/z 303 (M$^+$, 100), 246 (M$^+$ − ^{t}Bu, 100), 190 (^{t}BuGaS$_2$, 47), 119 (S$_2$CNMe$_2$, 20), 88 (SCNMe$_2$, 72), 69 (Ga, 58), 57 (^{t}Bu, 12). IR (cm^{-1}): 2704 (s), 1516 (m), 1465 (s), 1399 (s), 1260 (s), 1153 (m), 1096 (w), 1015 (m), 984 (s), 892 (s), 871 (s), 810 (m), 656 (w), 579 (m). ^{1}H NMR (C$_6$D$_6$): δ 2.46 (6H, s, NCH_3), 1.48 [18H, s, C(CH_3)$_3$]. ^{13}C NMR (C$_6$D$_6$): δ 42.1 (NCH$_3$), 30.7 [C(CH$_3$)$_3$], 26.1 [C(CH$_3$)$_3$].

(^{t}Bu)Ga(S$_2$CNMe$_2$)$_2$ (2). Yield: ca. 10%. Mp: 353 °C dec. MS (EI, %): m/z 309 (M$^+$ − ^{t}Bu, 100), 190 [(^{t}Bu)GaS$_2$, 18], 88 (SCNMe$_2$, 65), 69 (Ga, 58), 57 (^{t}Bu, 12). IR (cm^{-1}): 1511 (w), 1388 (s), 1260 (m), 1096 (w), 1014 (m), 984 (s), 866 (w), 799 (w). ^{1}H NMR (C$_6$D$_6$): δ 2.55 (12H, s, NCH_3), 1.71 [9H, s, C(CH_3)$_3$]. ^{13}C NMR (C$_6$D$_6$): δ 202.6 (CN), 43.6 (NCH$_3$), 30.8 [C(CH$_3$)$_3$], 30.4 [C(CH$_3$)$_3$].

Synthesis of (^{t}Bu)$_2$Ga(S$_2$CNEt$_2$) (3) and (^{t}Bu)Ga(S$_2$-CNEt$_2$)$_2$ (4). The reaction between [(^{t}Bu)$_2$Ga(μ-Cl)]$_2$ (0.88 g, 4.0 mmol) and Na(S$_2$CNEt$_2$) (0.86 g, 5.0 mmol) was carried out in a manner similar to that used for compounds **1** and **2**. The sublimate (40 °C, 10^{-2} Torr) was recrystallized in methylene chloride which gave clear, platelike crystals of (^{t}Bu)$_2$Ga-(S$_2$CNEt$_2$) (**3**). The residue remaining after sublimation, (^{t}Bu)Ga(S$_2$CNEt$_2$)$_2$ (**4**), was also isolated.

(^{t}Bu)$_2$Ga(S$_2$CNEt$_2$) (3). Yield: ca. 75%. MS (EI, %): m/z 331 (M$^+$, 5), 274 (M$^+$ − ^{t}Bu, 100), 218 (M$^+$ − 2^{t}Bu + H, 100), 116 (SCNEt$_2$, 60), 69 (Ga, 25), 57 (^{t}Bu, 10). IR (cm^{-1}): 1501 (m), 1358 (m), 1290 (s), 1276 (m), 1204 (m), 1148 (m), 1096 (s), 1071 (w), 999 (w), 917 (m), 876 (w), 839 (s), 813 (m), 784 (m), 750 (w), 651 (w). ^{1}H NMR (C$_6$D$_6$): δ 3.19 [4H, q, J(H−H) = 7.13 Hz, CH_2CH$_3$], 1.47 [18H, s, C(CH_3)$_3$], 0.77 [6H, t, J(H−

(38) Dunn, R. *Carbon Disulfide in Organic Chemistry*; Ellis Horwood: Chichester, England, 1989; pp 226−315.
(39) (a) Kovar, R. A.; Derr, H.; Brandau, D.; Callaway, J. O. *Inorg. Chem.* **1975**, *14*, 2809. (b) Schwering, H.-U.; Jungk, E.; Weidlein, J. J. *Organomet. Chem.* **1975**, *91*, C4.
(40) Kovar, R. A.; Loaris, G.; Derr, H.; Callaway, J. O. *Inorg. Chem.* **1974**, *13*, 1476.
(41) Cleaver, W. M.; Barron, A. R. *Chemtronics* **1989**, *4*, 146.

H) = 7.13 Hz, CH$_2$C*H$_3$*]. ^{13}C NMR (C$_6$D$_6$): δ 188.0 (*C*N), 47.7 (*C*H$_2$CH$_3$), 30.7 [*C*(CH$_3$)$_3$], 29.5 [C(*C*H$_3$)$_3$], 12.1 (CH$_2$*C*H$_3$).

(ᵗ**Bu)Ga(S$_2$CNEt$_2$)$_2$ (4).** Yield: ca. 10%. Mp: 351 °C dec. MS (EI, %): *m/z* 365 (M$^+$ − ᵗBu, 5), 218 (GaS$_2$CNEt$_2$ +H, 5), 148 (S$_2$CNEt$_2$, 1), 116 (SCNEt$_2$, 100), 57 (ᵗBu, 15). IR (cm^{-1}): 3391 (w), 2704 (s), 1650 (m), 1496 (s), 1429 (s), 1353 (s), 1265 (s), 1209 (s), 1148 (s), 1091 (s), 1071 (s), 1015 (w), 917 (s), 841 (s), 805 (m), 656 (m). ^{1}H NMR (C$_6$D$_6$): δ 3.25 [8H, q, *J*(H−H) = 7.20 Hz, C*H$_2$*CH$_3$], 1.71 [9H, s, C(C*H$_3$*)$_3$], 0.787 [12H, t, *J*(H−H) = 7.20 Hz, CH$_2$C*H$_3$*]. ^{13}C NMR (C$_6$D$_6$): δ 199.2 (*C*N), 49.1 (*C*H$_2$CH$_3$), 30.8 [*C*(CH$_3$)$_3$], 30.1 [C(*C*H$_3$)$_3$], 12.3 (CH$_2$*C*H$_3$).

Synthesis of (ᵗBu)$_2$Ga[S$_2$CN(ⁿPr)$_2$] (5) and (ᵗBu)Ga-[S$_2$CN(ⁿPr)$_2$]$_2$ (6). The reaction between [(ᵗBu)$_2$Ga(μ-Cl)]$_2$ (0.40 g, 1.8 mmol) and Na[S$_2$CN(ⁿPr)$_2$] (0.16 g, 8.7 mmol) was carried out in a manner identical to that used for compounds **1** and **2**. Removal of all volatiles gave a clear oil which was determined to contain a mixture of two products: (ᵗBu)$_2$Ga(S$_2$CNⁿPr$_2$) (**5**) and (ᵗBu)Ga(S$_2$CNⁿPr$_2$)$_2$ (**6**).

(ᵗ**Bu)$_2$Ga(S$_2$CNⁿPr$_2$) (5).** Yield: ca. 45%. MS (EI, %) *m/z* 302 (M$^+$ − ᵗBu, 100), 246 (M$^+$ − 2 ᵗBu, 35), 144 (GaS$_2$C, 30), 102 (HNPr$_2$, 5), 57 (ᵗBu, 15). IR (cm^{-1}): 3416 (w), 2761 (s), 2694 (m), 1685 (s), 1680 (m), 1511 (w), 1465 (s), 1429 (s), 1358 (s), 1342 (s), 1306 (s), 1245 (m), 1199 (m), 1148 (s), 1091 (s), 1030 (s), 1015 (s), 974 (m), 892 (s), 861 (m), 810 (s), 745 (s), 605 (m). ^{1}H NMR (C$_6$D$_6$): δ 3.25 [4H, m, *J*(H−H) = 6.07 Hz, NC*H$_2$*], 1.47 [18H, s, C(C*H$_3$*)$_3$], 1.39 [4H, m, *J*(H−H) = 6.07 Hz, NCH$_2$C*H$_2$*], 0.60 [6H, t, *J*(H−H) = 6.07 Hz, NCH$_2$CH$_2$C*H$_3$*]. ^{13}C NMR (C$_6$D$_6$): δ 198.0 (*C*N), 54.7 (N*C*H$_2$), 30.4 [*C*(CH$_3$)$_3$], 26.0 [C(*C*H$_3$)$_3$], 20.7 (NCH$_2$*C*H$_2$), 11.3 (NCH$_2$CH$_2$*C*H$_3$).

(ᵗ**Bu)Ga(S$_2$CNⁿPr$_2$)$_2$ (6).** Yield: ca. 45%. Mp: 288 °C dec. MS (EI, %) *m/z* 421 (M$^+$ − ᵗBu, 5), 302 (M$^+$ − S$_2$CNⁿPr$_2$, 80), 246 (M$^+$ − ᵗBu − S$_2$CNⁿPr$_2$, 30), 178 (S$_2$CNⁿPr$_2$, 5). IR (cm^{-1}): 2761 (s), 2730 (s), 2704 (s), 1957 (m), 1491 (w), 1424 (m), 1363 (s), 1301 (s), 1260 (m), 1235 (s), 1199 (s), 1148 (w), 1091 (s), 1030 (m), 1015 (s), 989 (s), 943 (s), 892 (s), 861 (s), 799 (m), 753 (s), 656 (m), 625 (s), 605 (s), 579 (s). ^{1}H NMR (C$_6$D$_6$): δ, 3.32 [8H, m, *J*(H−H) = 7.44 Hz, NC*H$_2$*], 1.72 [9H, s, C(C*H$_3$*)$_3$], 1.41 [8H, t, *J*(H−H) = 7.44 Hz, NCH$_2$C*H$_2$*], 0.62 [12H, t, *J*(H−H) = 7.44 Hz, NCH$_2$CH$_2$C*H$_3$*]. ^{13}C NMR (C$_6$D$_6$): δ 202.1 (*C*N), 56.3 (N*C*H$_2$), 30.8 [*C*(CH$_3$)$_3$], 26.4 [C(*C*H$_3$)$_3$], 20.8 (NCH$_2$*C*H$_2$), 11.4 (NCH$_2$CH$_2$*C*H$_3$).

(ⁿ**Bu)$_2$Ga(S$_2$CNMe$_2$) (7).** A solution of [(ⁿBu)$_2$Ga(μ-Cl)]$_2$ (1.0 g, 4.58 mmol) in hexane (10 mL) was added to a slurry of Na-(S$_2$CNMe$_2$) (0.60 g, 4.16 mmol) in hexane (30 mL) with continuous stirring. The resulting reaction mixture was allowed to stir for 30 min, then was heated to reflux overnight (10 h). This was then filtered and the filtrate removed of its volatiles to leave a mixture of the 1:1 and 2:1 products in the ratio 9:1. This compound was found to decompose after several hours exposure to air. Yield: ca. 95%. MS (EI, %) *m/z* 309 (M$^+$ − 2 ⁿBu + S$_2$CNMe$_2$, 100), 246 (M$^+$ − ⁿBu, 95) 190 (M$^+$ − 2 ⁿBu, 30), 120 (S$_2$CNMe$_2$, 20). IR (cm^{-1}, neat): 2952 (w), 2916 (w), 1949 (m), 1513 (m), 1455 (s), 1389 (m), 1258 (s), 1062 (w), 858 (m), 800 (w), 680 (m), 662 (s). ^{1}H NMR (C$_6$D$_6$): δ 2.47 [6H, s, N(C*H$_3$*)$_2$], 1.82 [4H, m, *J*(H−H) = 5.80 Hz, GaC*H$_2$*], 1.51 [4H, m, *J*(H−H) = 5.80 Hz, Ga−CH$_2$C*H$_2$*], 1.03 [10H, m, *J*(H−H) = 5.8 Hz, Ga−CH$_2$CH$_2$C*H$_2$*C*H$_3$*]. ^{13}C NMR (C$_6$D$_6$): δ 201.4 (*C*N), 42.0 [*N*(CH$_3$)$_2$], 29.8 (Ga−*C*H$_2$), 28.3 (Ga−CH$_2$*C*H$_2$), 17.1 (Ga−CH$_2$CH$_2$*C*H$_2$), 14.7 (Ga−CH$_2$CH$_2$CH$_2$*C*H$_3$).

(ˢᵉᶜ**Bu)$_2$Ga(S$_2$CNMe$_2$) (8).** A solution of [(ˢᵉᶜBu)$_2$Ga(μ-Cl)]$_2$ (1.0 g, 4.58 mmol) in hexane (10 mL) was added to a slurry of Na(S$_2$CNMe$_2$) (0.60 g, 4.16 mmol) with continuous stirring. The resulting reaction mixture was allowed to stir for 30 min, then was heated to reflux overnight (10 h). This was then filtered and the filtrate removed of its volatiles to leave a mixture of the 1:1 and 2:1 products in the ratio 9:1. Yield: ca. 95%. MS (EI, %) *m/z* 246 (M$^+$ − ˢBu, 95) 190 (M$^+$ − 2 ˢBu, 20), 88 (SCNMe$_2$, 100), 69 (Ga, 22), 57 (ᵗBu, 17). IR (cm^{-1}, neat): 2940 (m), 2851 (s), 2710 (s), 2630 (m), 1964 (m), 1520 (m), 1455 (s), 1389 (s), 1244 (s), 1135 (m), 1060 (m), 1030 (s), 982 (m), 793 (m). ^{1}H NMR (C$_6$D$_6$): δ 2.49 [6H, s, N(C*H$_3$*)$_2$], 1.96 [2H, m, *J*(H−H) = 7.50 Hz, C*H$_2$*CH$_3$], 1.86 [2H, m, *J*(H−H) = 7.50 Hz, C*H$_2$*CH$_3$], 1.54 [3H, d, *J*(H−H) = 3.03 Hz, CH(C*H$_3$*)], 1.52 [3H, d, *J*(H−H) = 3.03 Hz, CH(C*H$_3$*)], 1.34 [1H, m, *J*(H−H) = 7.50 Hz, Ga−C*H*], 1.33 [1H, m, *J*(H−H) = 7.50 Hz, Ga−C*H*], 1.17

[3H, t, *J*(H−H) = 7.3 Hz, CH$_2$C*H$_3$*]. ^{13}C NMR (C$_6$D$_6$): δ 201.3 (*C*N), 42.0 [*N*(CH$_3$)$_2$], 29.70 (*C*H$_2$CH$_3$), 29.68 (CH$_2$*C*H$_3$), 27.3 (Ga-*C*H), 27.2 (Ga-*C*H), 18.7 [CH(*C*H$_3$)], 15.7 (CH$_2$*C*H$_3$).

Volatility Studies. The thermogravimetric and differential thermal analyses for compounds **1**−**8** were measured on a Seiko 200 TG/DTA instrument. Generally 5−7 mg of sample was used with an argon flow rate of 300 mL·min^{-1}. Isothermal conditions were used to determine the ΔH_v and ΔS_v for compounds **1**, **3**, **5**, **7**, and **8** in a manner previously described in detail.[15] Briefly, the temperature was ramped to a desired value, the mass loss monitored over a 10-min period at constant temperature, and then the temperature was ramped to the next measurement value. The temperature ranges used are given in Table 2. The ΔH_f for compounds **1** and **3** were determined using differential thermal analysis with indium metal as a reference.[42] The areas under the endothermic thermal events were measured for each compound, and the ΔH_f was then calculated using the area found for the same mass of In.

Chemical Vapor Deposition. The chemical vapor deposition studies described herein were performed in a horizontal flow hot wall CVD chamber, as reported previously.[2d] All depositions were carried out under an inert Ar atmosphere with a 100 mL·min^{-1} flow rate or under low pressure (10^{-4} Torr). GaAs [100] substrates were used and were etched prior to use in a 1:1:500 solution of H$_2$SO$_4$:H$_2$O$_2$:H$_2$O, rinsed in deionized water, passivated in a 20% ammonium sulfide solution[43] rerinsed in deionized water, and then dried under nitrogen. Previously described procedures for the CVD runs were followed.[2d] Typical precursor and deposition temperatures are summarized in Table 3.

Film Characterization. X-ray diffraction studies were performed using a Siemens D5000 diffractometer with graphite monochromated Cu Kα radiation (λ = 1.540 59 Å). The unit cell of the resulting diffraction pattern was determined by X-draw.[44] The composition of the films was measured using a Cameca SX-50 electron microprobe, relative to calibration standards. Scanning electron microscopy (SEM) was performed to determine the surface features, on either a JEOL 5300 SEM or a 6320F FESEM. TEM samples were obtained by growing thin films on single-crystal NaCl substrates over short deposition times (ca. 8 min). Immersing the NaCl substrates in water allowed the separation of the free films which were subsequently placed on copper TEM grids. Samples were then dried overnight and sputtered with carbon prior to analysis. A JEOL 2010 TEM operating at 200 keV was used. XPS measurements were performed on a PHI 5700 system using a lens focus area of 1 mm with an aluminum anode at 15 kV and 28 mA and a base pressure of 10^{-10} Torr. Sample temperature during analysis was either room temperature (ca. 20 °C) or 600 °C. The higher temperature study being conducted in situ after the sample had been heated for 10 min. All binding energies studied were referenced to graphitic carbon. All signals were fitted with the minimum number of peaks that provides the best fit. SIMS measurements were obtained on a PHI 6600 instrument using a Cs$^+$ source at 5 keV, with an ion current of 10−20 nA, and a 500 μm spot size and a sputter angle of 74.8 °. The Gaussian−Lorentz least-squares curve fit was done using Multi-Pak v.5 software package for the PHI 5700 ESCA operating system.

Crystallographic Studies. Crystals of compounds **1** and **3** were sealed in a glass capillary under argon and mounted on the goniometer of a Enraf-Nonius CAD-4 automated diffractometer with graphite-monochromated Mo Kα radiation (λ = 0.71073 Å). Data collection and cell determinations were performed in a manner previously described,[45] using the θ/2θ scan technique. Pertinent details are given in Table 6. The

(42) See ref 17, Chapter 7, p 252.
(43) Yablonovitch, E.; Sandroff, C. J.; Bhat, R.; Gmitter, T. *Appl. Phys. Lett.* **1987**, *51*, 439.
(44) Shareware: Grubbs, D. 1990.
(45) Mason, M. R.; Smith, J. M.; Bott, S. G.; Barron, A. R. *J. Am. Chem. Soc.* **1993**, *115*, 4971.

Table 6. Summary of X-ray Diffraction Data

compound	(^{t}Bu)$_2$Ga(S$_2$CNMe$_2$) (**1**)	(^{t}Bu)$_2$Ga(S$_2$CNEt$_2$) (**3**)
empirical formula	C$_{11}$H$_{24}$GaNS$_2$	C$_{13}$H$_{28}$GaNS$_2$
cryst size, mm	0.08 × 0.22 × 0.48	0.07 × 0.13 × 0.16
cryst syst	monoclinic	monoclinic
space group	P2$_1$/n	P2$_1$/c
a, Å	15.857(2)	11.101(2)
b, Å	6.464(2)	8.840(1)
c, Å	15.904(2)	19.305(4)
β, deg	90.28(9)	105.12(2)
V, Å^3	1630.4(5)	1828.9(5)
Z	4	4
D(calcd), g/mL	1.239	1.207
μ, cm^{-1}	19.04	17.07
temp, K	298	298
2θ range, deg	3.0−44.0	3.0−44.0
no. of reflcns collected	2292	2551
no. of indep reflcns	2201	2420
no. of obsd reflcns	780 ($|F_o| > 6.0\sigma\,|F_o|$)	821 ($|F_o| > 6.0\sigma\,|F_o|$)
weighting scheme	w^{-1} = 0.04($|F_o|$)^2 + $\sigma(|F_o|)^2$	w^{-1} = 0.04($|F_o|$)^2 + $\sigma(|F_o|)^2$
R	0.0603	0.0474
R_w	0.0669	0.0551
largest diff peak, e Å^{-3}	0.41	0.65

structures were solved by direct methods (SHELX86).[46] The models were refined using full-matrix least squares techniques. All non-hydrogen atoms were refined anisotropically. Hydrogen atoms were included and constrained to "ride" upon the appropriate atoms [d(C−H) = 0.95 Å, U(H) = 1.3B_{eq}(C)]. All computations other than those specified were performed using MolEN.[47] A summary of cell parameters, data collection, and structure solution is given in Table 6. Scattering factors were taken from ref 48.

Supporting Information Available: Full listings of bond length and angles, anisotropic thermal parameters, and hydrogen atom parameters and tables of calculated and observed structure factors. This material is available free of charge via the Internet at http://pubs.acs.org.

CM9903632

(46) SHELX86: Sheldrick, G. M. In *Crystallographic Computing*; Sheldrick, G. M., Kruger, C., Goddard, R., Eds.; Oxford University Press: London, 1985; pp 184−189.

(47) MolEN: Enraf-Nonius. *MolEN, An interactive Structure Solution Procedure*; Enraf-Nonius, Delft, The Netherlands, 1990.
(48) *International Tables for X-ray Crystallography*; Kynoch Press: Birmingham, England, 1974; Vol. 4.